

RSC Advances



This is an *Accepted Manuscript*, which has been through the Royal Society of Chemistry peer review process and has been accepted for publication.

Accepted Manuscripts are published online shortly after acceptance, before technical editing, formatting and proof reading. Using this free service, authors can make their results available to the community, in citable form, before we publish the edited article. This *Accepted Manuscript* will be replaced by the edited, formatted and paginated article as soon as this is available.

You can find more information about *Accepted Manuscripts* in the [Information for Authors](#).

Please note that technical editing may introduce minor changes to the text and/or graphics, which may alter content. The journal's standard [Terms & Conditions](#) and the [Ethical guidelines](#) still apply. In no event shall the Royal Society of Chemistry be held responsible for any errors or omissions in this *Accepted Manuscript* or any consequences arising from the use of any information it contains.



Journal Name

ARTICLE

Design specific mechanistic regulation of sensing phenomenon of two Schiff bases towards Al³⁺ †

Received 00th January
20xx,
Accepted 00th January
20xx

DOI: 10.1039/x0xx00000x

www.rsc.org/

Shweta,^a Neeraj,^a Sharad Kumar Asthana,^a Rakesh K. Mishra^b and K.K. Upadhyay^{a*}

We report herein two optical probes (**R1** and **R2**) for the fluorogenic detection of Al³⁺ at the level of 10⁻⁸ M. The **R1** and **R2** were synthesized by simple schiff base condensation of 4-amino-3-hydroxy-1-naphthalene sulfonic acid with 5-bromosalicylaldehyde and 2-hydroxy-1-naphthaldehyde respectively. The same were characterized by various spectroscopic techniques. The **R1** and **R2** both underwent fluorescence emission upon their respective interactions with Al³⁺ in ethanol : water mixture (4: 1, v/v). The binding modes of receptors with Al³⁺ were studied through ¹H NMR, Job's plot, HR-MS as well as through binding constant determination involving fluorescence titration data. The quenching of –C=N isomerization and of photoinduced electron transfer (PET) seem to be responsible for fluorogenic switch on situation of **R1** and **R2** with Al³⁺. At the same time the excited state intramolecular proton transfer (ESIPT) also plays important role in the ratiometric fluorescent response of **R2** which is a consequence of a minor structural variation in **R1** by removing the bromophenyl moiety with the naphthalene one. The mechanistic aspects of the sensing phenomenon were discussed in terms of ¹H NMR titration as well as theoretical calculations at the density functional level.

Introduction

The long lasting toxic impact of various biologically and environmentally relevant metal ions in biological systems have attracted increasing interest for the development of opto-chemical (optodes) probes. Among these the fluorescent ones have attracted much attention of chemists due to their high sensitivity and instantaneous response.¹ At the same time the same have also been exploited for the purposes of bio-assay in the form of fluorescent marker.² Fluorescence offers significant advantages over other methods for analyte detection and corresponding measurements. The Al (III) is the third most abundant metal ion in the earth's crust and it is known for its toxic behavior in biological/environmental systems.³ It is used in our daily live, often as packaging materials. The main reason for occurrence of Al³⁺ in environment is its leaching from soil by acid rain and human activities.^{4a-b} The aluminium toxicity involves damage of human tissues and cells, causing health problems such as dementia, microcytic hypochromic anemia, Al-related bone disease (ARBD), encephalopathy, neuronal myopathy etc.⁵ The same also known to damage the central nervous system.⁵

Moreover, aluminium toxicity is also linked to several neurodegenerative diseases like Alzheimer's and Parkinson's disease.^{6a-c} According to World Health Organization (WHO) the estimated provisional tolerable weekly intake of aluminum (PTWI) for healthy individuals is 7 mg per kg body weight.⁷ Therefore, it is mandatory to monitor the concentration of Al³⁺ ions in the environment to maintain good human health. Till date, various 'turn-on' fluorescent chemosensors have been reported where the basic fluorophore used are hydrazone, pyrene, 8-hydroxyquinoline, hydroxyflavone, benzamidazoline etc.^{8a-e}

Our own group has reported a few chemosensors for Al³⁺ involving simple synthetic approaches with low detection limits.^{9a-c} Present work is yet another addition to our existing stock with unraveling of an interesting mechanistic approach viz. excited state intramolecular proton transfer (ESIPT), of **R2** towards Al³⁺. In recent years a number of workers have reported a variety of schiff bases as a chemosensors particularly the fluorescent ones for Al³⁺.^{10a-d} The majority among them are of off-on/on-off sensors. Nevertheless, the ratiometric fluorescent sensors for Al³⁺ are rare in the form of Schiff bases.¹¹ Present report has its own worth in the sense that the same presents two sensors first the **R1** as off/on sensor and second the **R2** is ESIPT blended ratiometric fluorescent sensor (Fig.1). Chemosensors with ESIPT-based phenomena are supposed to be more suitable as their dual peak is more convenient for the optical monitoring of concerned analyte. These chemosensors generally contain a five/six membered hydrogen bonded ring structure exhibiting high speed intramolecular proton transfer in their excited

* Corresponding author: ^aDepartment of Chemistry (Centre of Advanced Study), Institute of Science, Banaras Hindu University, Varanasi, Uttar Pradesh-221005, India. Tel: +91 542 670 2488; E-mail: drkaushalbhhu@yahoo.co.in; kku@bhu.ac.in

^b Photosciences and Photonics, Chemical Sciences and Technology Division, CSIR-National Institute for Interdisciplinary Science and Technology, Triruvananthapuram-695019, India.

† Electronic Supplementary Information (ESI) available: ¹H NMR, ¹³C NMR, IR, mass spectrum of **R1**, **R2** and Al³⁺ complex of **R1** and **R2**. See DOI: 10.1039/x0xx00000x

state resulting into a very weak or no fluorescence.¹² The same undergo deprotonation upon their interaction with a particular analyte, causing inhibition of ESIPT and enhancement of their fluorescence intensity.^{13a-c} The compounds with $-C=N$ isomerization and finite possibility of photoinduced electron transfer (PET) phenomenon are often weak/non-fluorescent.^{14a-c} If there is an orbital of ionophore in between the HOMO and LUMO of fluorophore an electron from the HOMO of the ionophore may be transferred to the HOMO of the excited fluorophore through space. The same may also occur from the LUMO of an excited fluorophore to the empty orbital of the ionophore. The same results into the virtual quenching of the fluorescence of the receptor is termed as photo-induced electron transfer (PET).¹⁵ However the metal complexes of the above type of ligands exhibit good extent of fluorescence dramatically due to suppression of $-C=N$ isomerization as well as of PET phenomenon.^{16a-c}

We are presenting two optical sensors **R1** and **R2** upon the skeleton of naphthalene sulfonic acid with non-fluorescent and weak fluorescent properties respectively. The **R1** and **R2** both responded well selectively towards Al^{3+} in fluorogenic mode. Nevertheless, the response of **R2** was in ratiometric mode due to significant extent of excited state intramolecular proton transfer (ESIPT) phenomenon into the same. Though structurally both **R1** and **R2** are expected to involve ESIPT phenomenon as they possess similar structure. Here our designed strategy became important. In **R2** we incorporated a naphthalene moiety in the place of bromophenyl which ultimately lead to over stability of the keto form in **R2** as compared to **R1** (under the heading of DFT) which finally lead to the significant extent of ESIPT in **R2**.

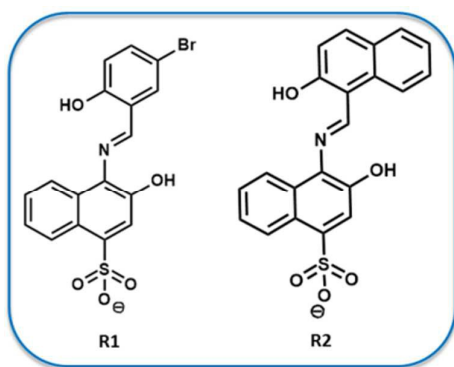


Fig. 1 Molecular Structure of receptors **R1** and **R2**.

Experimental Section

The synthesis of receptors **R1** and **R2** have been shown in Scheme 1. 1.0 mmol absolute ethanolic solution of 5-bromosalicylaldehyde and 2-hydroxy-1-naphthaldehyde respectively were separately added to an equimolar absolute

ethanolic solution of 4-amino-3-hydroxy-1-naphthalene sulphonic acid having 2 mmol triethylamine. The reaction mixtures were stirred separately overnight at room temperature resulting into yellow solid compounds followed by their filtration, washing with ethanol and drying under vacuum. The receptors were characterized by FT-IR, 1H & ^{13}C NMR along with HRMS spectral studies (ESI⁺; Figure S1-S4 & S5-S8).

Spectroscopic characterization data of **R1**

Yield: 80%; **IR/cm⁻¹:** 3056, 2731, 1610, 1561, 1506, 1476, 1421, 1391, 1340, 1299, 1267, 1227, 1191, 1142, 1097, 1039, 985, 965, 910, 889, 845, 764, 643, 622, 589, 561, 540; **1H NMR (300 MHz, DMSO-*d*₆, TMS):** δ ppm = 13.44 (s, $-OH^1$, 1H), 10.19 (s, $-OH^2$, 1H), 9.12 (s, $-CH=N-$, 1H), 8.75-8.73 (d, Ar-H, 1H), 7.94-7.86 (m, Ar-H, 3H), 7.57-7.32 (m, Ar-H, 3H), 6.97 (s, $-Ar-H$, 1H), 3.09-3.02 (q, $-CH_2$, 6H), 1.16-1.11 (t, $-CH_3$, 9H); **^{13}C NMR (75 MHz, DMSO-*d*₆, TMS):** δ ppm = 166.20, 159.49, 143.20, 143.00, 135.31, 133.60, 129.77, 127.99, 127.76, 126.31, 124.02, 122.97, 121.59, 121.31, 119.08, 117.91, 109.95, 45.77, 8.60; **HRMS:** m/z calculated for $C_{17}H_{12}BrNO_5S$ = 420.96196; found = 421.96887.

Spectroscopic characterization data of **R2**

Yield: 76%; **IR/cm⁻¹:** 3045, 1620, 1605, 1560, 1506, 1477, 1389, 1347, 1333, 1272, 1225, 1192, 1101, 1040, 968, 925, 852, 824, 768, 735, 657, 648, 637, 595, 544, 435; **1H NMR (300 MHz, DMSO-*d*₆, TMS):** δ ppm = 16.13 (s, $-OH^1$, 1H), 10.41 (s, $-OH^2$, 1H), 9.92 (s, $-CH=N-$, 1H), 8.81-8.78 (d, Ar-H, 1H), 8.21-7.99 (t, Ar-H, 1H), 7.98-7.93 (m, Ar-H, 3H), 7.84-7.79 (m, Ar-H, 1H), 7.56-7.49 (m, Ar-H, 2H), 7.40-7.32 (m, Ar-H, 2H), 7.12-7.09 (d, Ar-H, 1H) 3.09-3.05 (q, $-CH_2$, 6H), 1.17-1.13 (t, $-CH_3$, 9H); **^{13}C NMR (75 MHz, DMSO-*d*₆, TMS):** δ ppm = 168.99, 161.99, 144.61, 143.04, 138.49, 136.32, 132.97, 129.34, 129.19, 128.88, 128.33, 128.01, 126.76, 124.94, 124.15, 123.45, 123.25, 121.79, 120.84, 119.53, 108.52, 45.83, 8.65; **HRMS:** m/z calculated for $C_{21}H_{14}NO_5S$ = 392.05982; found = 392.05868.

Synthesis of Al^{3+} complex with **R1** & **R2**

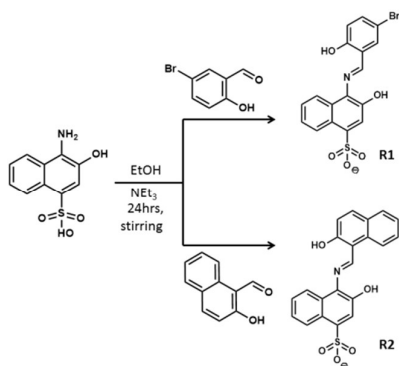
A 10 mL methanolic solution of $AlCl_3$ (0.5 mmol) was added separately to a magnetically stirred 10 mL methanolic solution of **R1**, (0.5 mmol) and **R2** (0.5 mmol) respectively. The reaction mixtures were stirred on ice bath for ~3h whereby an off white precipitate was formed in both cases. The same were filtered, washed with water several times followed by diethyl ether and finally dried under vacuum over anhydrous $CaCl_2$. The complexes were characterized by FT-IR, 1H & ^{13}C NMR along with HRMS spectral studies (ESI⁺; Figure S9-S12 & S13-S16).

Spectroscopic characterization data of $R1-Al^{3+}$

Yield: 84%; **IR/cm⁻¹:** 3430, 3011, 2921, 1619, 1526, 1438, 1423, 1359, 1241, 1174, 1161, 1136, 1046, 1002, 963, 833, 724, 659, 539; **¹H NMR (300 MHz, DMSO-*d*₆, TMS):** δ ppm = 10.18 (s, -OH², 1H), 9.09 (s, -CH=N-, 1H), 8.75-8.72 (d, Ar-H, 1H), 7.93-7.84 (m, Ar-H, 3H), 7.57-7.33 (m, Ar-H, 3H), 6.97 (s, Ar-H, 1H), 3.10-3.03 (q, -CH₂, 6H), 1.19-1.14 (t, -CH₃, 9H); **¹³C NMR (75 MHz, DMSO-*d*₆, TMS):** δ ppm = 166.24, 159.53, 143.22, 142.97, 138.48, 135.32, 133.31, 129.79, 127.77, 126.32, 124.05, 123.00, 121.11, 119.08, 117.92, 109.99, 45.77, 8.60; **HRMS:** *m/z* calculated for C₁₈H₁₆AlBrNO₇S⁻ = 495.96517; found = 495.96362.

Spectroscopic characterization data of R2-Al³⁺

Yield: 90%; **IR/cm⁻¹:** 3202, 1530, 1168, 1045, 750, 654; **¹H NMR (300 MHz, DMSO-*d*₆, TMS):** δ ppm = 10.80 (s, -NH-, 1H), 9.92 (s, -CH=N-, 1H), 8.81-8.73 (t, Ar-H, 1H), 8.21-8.19 (d, Ar-H, 1H), 7.98-7.94 (m, Ar-H, 3H), 7.84-7.79 (m, Ar-H, 1H), 7.53 (s, Ar-H, 2H), 7.41-7.12 (m, Ar-H, 2H), 7.09 (d, Ar-H, 1H), 3.10-3.05 (q, -CH₂, 6H), 1.18-1.13 (t, -CH₃, 9H); **¹³C NMR (75 MHz, DMSO-*d*₆, TMS):** δ ppm = 144.53, 143.22, 136.21, 132.95, 129.26, 129.09, 128.25, 128.04, 126.66, 124.12, 123.35, 123.09, 121.71, 120.73, 119.51, 117.93, 108.47, 45.69, 8.57; **HRMS:** *m/z* calculated for C₂₂H₁₉AlNO₇S⁻ = 468.07031; found = 468.06911.



Scheme 1 Synthesis of receptors **R1** and **R2**.

Results and discussion

The photophysical behavior of **R1** and **R2** were initially evaluated through naked eye and UV-visible spectral analysis. Both receptors were soluble in common organic solvents; hence their UV-vis. studies were investigated in 10 μ M ethanol–water mixture (4: 1, v/v).

The **R1** showed absorption bands at \sim 301 nm, \sim 375 nm as well as \sim 390 nm. Out of these the \sim 390 nm band was assigned

as the charge transfer band (n - π^*) on the similar line of earlier literature reports.^{9b, 17a-d}. The same underwent to a gradual bathochromic shift to \sim 450 nm with a small hump at \sim 476 nm upon addition of different aliquots of Al³⁺. At this stage the color of the solution became dark yellow from faint yellow (Fig. 2a). On the similar line of **R1**, the interaction of **R2** with Al³⁺ was also studied by UV-vis. titration. The **R2** showed a strong absorption band at \sim 447 nm and a shoulder at \sim 475 nm.

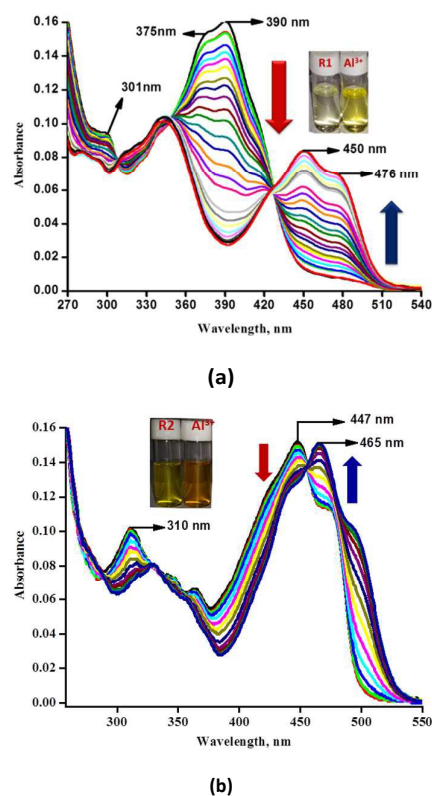


Fig. 2 Absorption titration profile in EtOH: H₂O mixture (4: 1, v/v) upon gradual addition of (a) Al³⁺ (0-4.0equiv.) in **R1** and (b) Al³⁺ (0-20.0equiv.) in **R2**

The concomitant additions of Al³⁺ to 10 μ M solution of **R2** in ethanol: water (4: 1, v/v) mixture lead to a red shift of 18 nm with a new peak at \sim 465 nm and a shoulder at \sim 492 nm and the color of **R2** changed from yellow to brownish yellow (Fig 2b). Thus, appearance of new bands as well as occurrence of isosbestic points clearly indicated the respective chemical interactions of **R1** and **R2** with Al³⁺.

The selectivity of **R1** and **R2** for Al³⁺ was checked over a wide range of cations through UV-vis. studies. The separate additions of 10 equiv. each of a number of cations viz., Al³⁺, Cr³⁺, Mn²⁺, Fe³⁺, Co²⁺, Ni²⁺, Cu²⁺, Zn²⁺, Cd²⁺, Hg²⁺ and Pb²⁺, Na⁺, K⁺, Ba²⁺, Ca²⁺, Mg²⁺ as their chloride salts were added in **R1** and **R2** separately. A few metal ions viz. Cu²⁺ and Fe³⁺ were able to perturb the UV-vis. spectral and naked-eye appearance of

R2 solution on the similar line of Al^{3+} (ESI[†]; Figure S17-S18) while in **R1**, Ni^{2+} , Cu^{2+} and Fe^{3+} were found to interfere (ESI[†]; Figure S19-S20). Hence **R1** and **R2** were not conclusive for any particular metal ion in their absorption mode.

Failure of **R1** and **R2** in their selective chromogenic responses against any particular cation prompted us for investigating their selectivity through fluorescence studies in ethanol: water (4:1, v/v). The **R1** was non-fluorescent upon its excitation at ~ 453 nm. However the concomitant additions of Al^{3+} (0-150 equiv.) to the **R1** solution lead a fully developed single band at ~ 537 nm with a remarkable fluorescence enhancement (Fig.3a). This fluorescence emission of **R1** in presence of Al^{3+} can be attributed to the quenching of $-\text{C}=\text{N}$ isomerization as well as hampering of PET phenomenon due to involvement of lone pair of nitrogen of $-\text{C}=\text{N}$ in the coordination with Al^{3+} (CHEF, chelation enhanced fluorescence).^{18a-b} At this juncture we observed bright yellow fluorescence under UV-light.

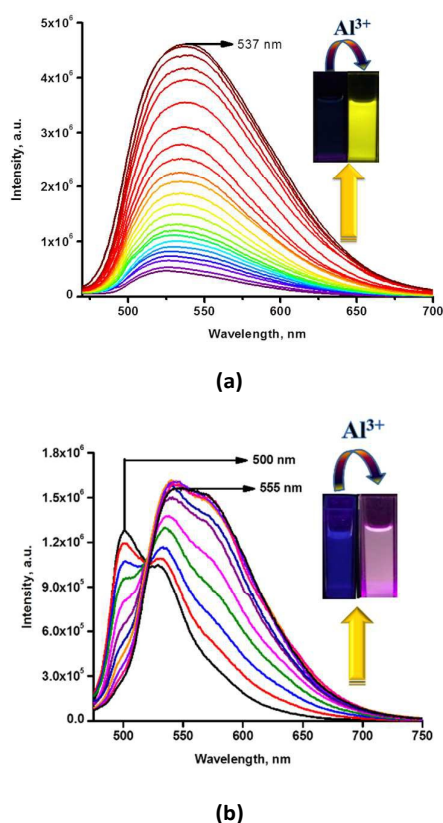


Fig. 3 Emission titration profile in 4: 1 (v/v); EtOH: H_2O upon concomitant addition of (a) Al^{3+} (0–150 equiv.) in **R1**; $\lambda_{\text{ex}}=453$ nm, (b) Al^{3+} (0–25 equiv.) in **R2**; $\lambda_{\text{ex}}=465$ nm.

On the other hand the **R2** itself was fluorescent and exhibited two emission bands at ~ 500 nm and ~ 528 nm respectively upon its excitation at ~ 465 nm. The dual emissive band of **R2** is the consequence of excited state intramolecular

proton transfer (ESIPT) phenomenon due to rapid exchange of proton between phenolic moiety situated at naphthol and imine nitrogen of aldimine group of **R2**. This type of behavior has already been mentioned in literature incorporating theoretical and experimental studies for the keto-enol tautomerization in the Schiff bases having 2-hydroxy naphthaldehyde as one component.¹⁹ The emission of **R2** at lower wavelength (~ 500 nm) was assigned to the enol form, while the keto form emits at the higher wavelength (~ 528 nm). Upon concomitant additions of Al^{3+} (0-25 equiv.) to **R2** solution we got fully developed emission band at ~ 555 nm with ratiometric red shift along with fluorescence enhancement. It is evident from the emission titration profile that there is a gradual decrease in enol band (~ 500 nm) and progressive increase in keto band (~ 528 nm) which subsequently resulted into a single broad band at ~ 555 nm (Fig 3b). This fluorescence augmentation in **R2** can be understood in terms of inhibition of $-\text{C}=\text{N}$ isomerization and PET as the result of effective chelation of **R2** with Al^{3+} (chelation enhanced fluorescence (CHEF). The same provides rigidity to **R2** resulting into planar orientation of the same and at this stage a light pink fluorescence under UV light was observed. The same observation was further supported by ^1H NMR titration and mass spectral studies also.

To check the fluorescence selectivity of **R1** and **R2** towards Al^{3+} , a range of cations *i.e.* Cr^{3+} , Mn^{2+} , Fe^{3+} , Co^{2+} , Ni^{2+} , Cu^{2+} , Zn^{2+} , Cd^{2+} , Hg^{2+} , Pb^{2+} , Na^+ , K^+ , Ba^{2+} , Ca^{2+} , Mg^{2+} as their chloride salts were added to **R1** and **R2** respectively. Only Al^{3+} lead fluorescence enhancement in **R1** which was visible as yellow fluorescence under UV-light (Fig. 4 & 5).

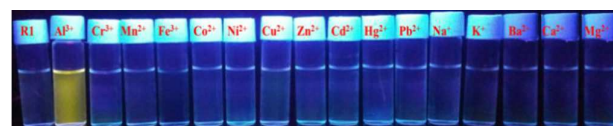


Fig. 4 Photograph of visual response of **R1** in presence of various metal ions (under UV-light).

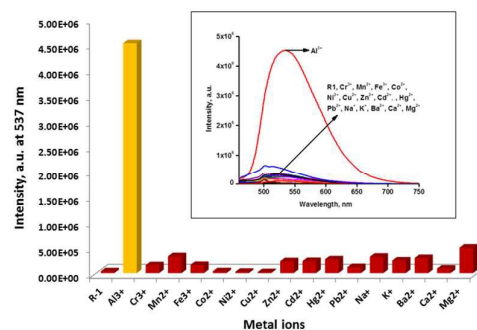


Fig. 5 Bar graph representation of **R1** with various metal ions. [Inset] Emission spectra of **R1** with various metal ions; $\lambda_{\text{ex}}=453$ nm.

On the other hand, **R2** underwent two types of modulation in its fluorescence characteristics. The first one was in the ratiometric terms with $\sim 55\text{nm}$ red shift upon the addition of Al^{3+} . Secondly, Fe^{3+} and Cu^{2+} were able to cause quenching of fluorogenic response of **R2**. (Fig.6 & 7).

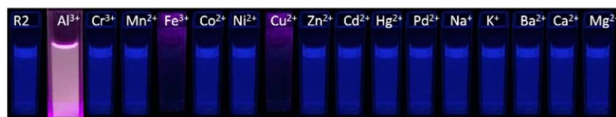


Fig. 6 Photograph of visual response of **R2** in presence of various metal ions (under UV-light).

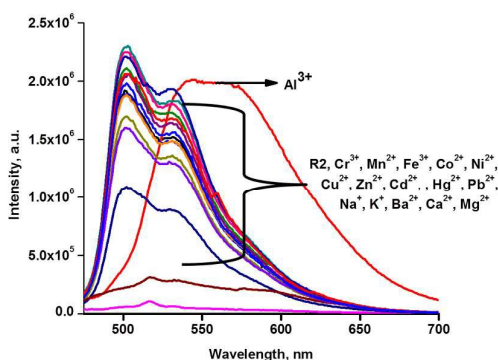
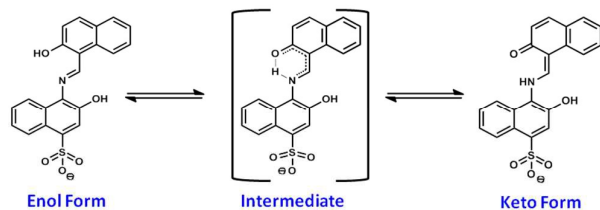


Fig. 7 Emission spectra of **R2** with various metal ions; $\lambda_{\text{exc}}=465\text{nm}$

The competition experiments were further performed to check the practical applicability of **R1** and **R2** as an Al^{3+} selective fluorescent probe. We took different metal ions in ethanol-water (4: 1, v/v) in presence of Al^{3+} . The Fe^{3+} and Cu^{2+} resulted into quenching in both the cases while rest of the metal ions didn't. The corresponding observation have been presented in the form of bar graph shown in the (ESI[†]; Figure S21-S22).

Since **R1** and **R2** both possess similar enol-imine structure, hence they are expected to undergo ESIPT through keto-enol tautomerism.^{20a-e} However, the emission spectra of **R1** and **R2** exhibited single and dual bands respectively in their fluorescence spectra (Fig.3a & 3b) which clearly indicated the enol-imine tautomerization to be operative only in **R2** [Scheme 2]



Scheme 2 Schematic representation of **R2** showing keto-enol form.

pH study

The pH value has great importance during the detection procedures for chemosensors having replaceable proton especially in protonic solvents. To determine the convenient pH conditions for the probes the emission intensity was investigated as the function of pH range 1.0 to 13.0. (ESI[†]; Figure S23-S24). It was observed that **R1** was almost nonresponsive while **R2** showed a noticeable response within pH range of 4.0-8.0 respectively. However both exhibited similar pattern upon the respective Al^{3+} additions in the pH range of 4.0-8.0. At $\text{pH}<4.0$ the intensities of **R1** and **R2** got diminished which can be understood in terms of competition between Al^{3+} and H^+ for nitrogen donor of aldimine $-\text{C}=\text{N}$. While at higher pH values ($\text{pH}>8.0$) the fluorescence got enhanced which can be understood in terms of extended conjugation in **R1** and **R2** as the result of deprotonation. Hence both **R1** and **R2** can be used for the detection of Al^{3+} within the pH range of 4.0-8.0.^{1, 21a-b}

The binding behavior of **R1** and **R2** with Al^{3+}

For having an idea about interaction of **R1** and **R2** with Al^{3+} , we did ^1H NMR titrations between the respective solutions of **R1** and **R2** (both 10 mM) separately in $\text{DMSO}-d_6$ and Al^{3+} as its chloride salt in D_2O . Fig. 8 clearly shows that **R1** exists in phenolic form showing $-\text{OH}^2$ at 10.16 δ ppm. The imine proton appears at 9.14 δ ppm while the $-\text{OH}^1$ showed its resonance at 13.45 δ ppm. Upon addition of 2 equiv. of Al^{3+} to **R1** the peak for $-\text{OH}^2$ shifted slightly up field while for $-\text{OH}^1$ became shorter and broader. Upon further increment of Al^{3+} there was complete disappearance of $-\text{OH}^1$ while the $-\text{OH}^2$ got shortened. Beside this, slight upfield shifting of $-\text{CH}=\text{N}$ proton was also observed. Hence the above ^1H NMR titration clearly supports effective binding of **R1** with Al^{3+} in enolic form.

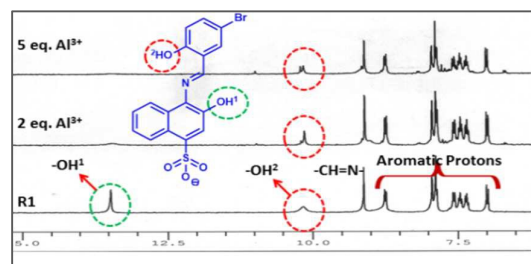


Fig. 8 ^1H NMR titration spectra of **R1** with Al^{3+} .

The **R2** exists in enolic form showing $-\text{OH}^1$ proton at 16.13 δ ppm, $-\text{OH}^2$ proton at 10.41 δ ppm and imine ($-\text{CH}=\text{N}$) proton at 9.92 δ ppm (Fig. 9).

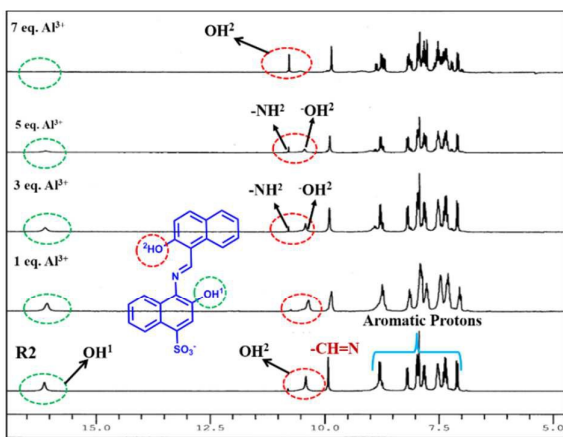


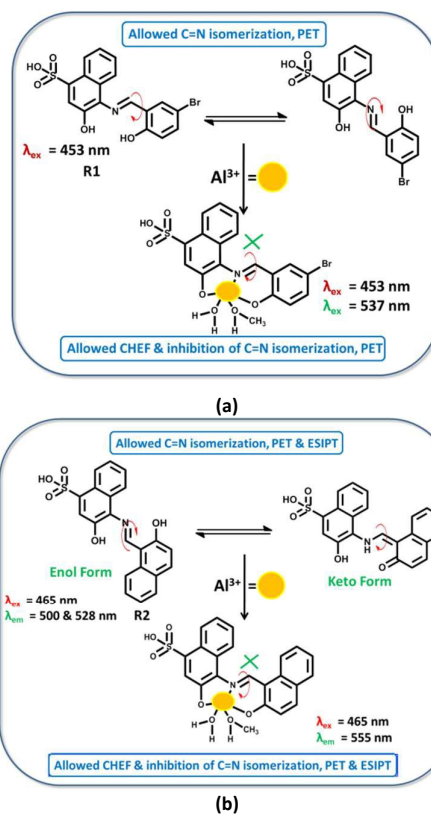
Fig. 9 ^1H NMR titration spectra of **R2** with Al^{3+} .

Upon concomitant additions of Al^{3+} into **R2**, finally deprotonation of $-\text{OH}^1$ took place. However, in due course of addition of Al^{3+} a peak started emerging ($-\text{NH}^2$) in the vicinity of $-\text{OH}^2$ which grew constantly. This strengthened our speculation regarding keto-enol tautomerization in **R2**. However after complete addition of Al^{3+} both the peaks ($-\text{NH}$ & $-\text{OH}$) became unified and finally observed at 10.776 ppm. Thus from these observations we can say that **R2** underwent into its enol form prior to its binding with Al^{3+} .

The separate job's plot experiments for **R1** and **R2** against Al^{3+} indicated the maxima at 0.5 which further indicated 1:1 stoichiometry in both the cases (ESI † ; Figure S25-S26). In addition to above studies the high resolution mass spectrometric studies were also performed in order to confirm the composition of the ensembles of Al^{3+} derived from **R1** and **R2** respectively. The mass spectrum of **R1**- Al^{3+} at m/z 495.96362 corresponds to $\text{C}_{18}\text{H}_{16}\text{AlBrNO}_7\text{S}^-$ and (ESI † ; Figure S4 & S12) on the similar line **R2**- Al^{3+} showed m/z at 468.06911 corresponds for $\text{C}_{22}\text{H}_{19}\text{AlNO}_7\text{S}^-$ (ESI † ; Figure S8 & S16) which again indicated a 1:1 binding of Al^{3+} with respective probes **R1** and **R2**.

The association constants of **R1** and **R2** towards Al^{3+} were evaluated from their respective fluorescence titration data and were found to be $(2.95 \pm 0.49) \times 10^5$ [$R^2 = 0.9973$] and $(4.06 \pm 0.89) \times 10^5$ [$R^2 = 0.9959$] respectively for **R1** and **R2** (ESI † ; Figure S27-S28). The lowest detection limits were worked out to be 3.00×10^{-8} M ($R^2 = 0.9977$) for **R1** and 2.35×10^{-8} M ($R^2 = 0.9813$) for **R2** with their respective linearity range of 8.5×10^{-6} M to 1.35×10^{-5} M and 0 M to 3.5×10^{-5} M (ESI † ; Figure S29-S30) using IUPAC method.^{22a-b}

Based on the above results from NMR titration, job's plot and HRMS spectral studies and binding constant calculation, the tentative binding modes of **R1** and **R2** with Al^{3+} have been shown in Scheme 3.



Scheme 3 Proposed sensing mechanism and binding mode of (a) **R1** and (b) **R2** with Al^{3+} .

Theoretical Calculations

The theoretical studies were also performed at the density functional level in order to fortify the informations regarding the structural details of the ensembles of Al^{3+} with **R1** and **R2** respectively. The calculations were carried out with Gaussian 09 programme and the structures were optimized in gaseous state using B3LYP/6-31G**.²³ The optimized structures of the receptors **R1** and **R2** along with their Al^{3+} complexes have been given in (ESI † ; Figure S31 & S32).

As it can be clearly seen in Fig 10 & 11 that the HOMO-LUMO energy gaps of **R1** and **R2** got shrunk upon their respective complexation with Al^{3+} . This clearly explained the observed bathochromic shifts in the UV-vis and fluorescence spectra of **R1** and **R2** upon the respective additions of Al^{3+} . The DFT calculations were helpful once again for having a plausible explanation for the operation of ESIPT phenomenon in **R1** and **R2** in a discriminative way. As we discussed above in the introduction that **R1** and **R2** both possess similar structure and hence possess finite possibility of intramolecular proton transfer in their excited state. We optimized both possible structures (**R1** and **R2**) i.e. enol and the keto forms through DFT calculations using B3LYP/6-31G** as the basis set. A comparison of the HOMO's of the keto forms of **R1** and **R2**

clearly indicates the over stability of the latter one over the previous one. Hence the operation of ESIPT is more likely in **R2** as compared to the **R1**.

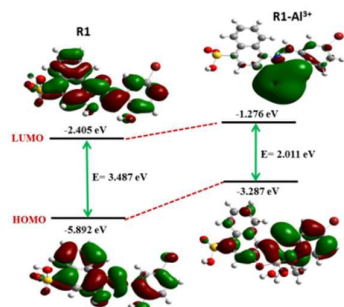


Fig.10 Energy level diagram for the frontier π -MOs of **R1** and **R1-Al³⁺**.

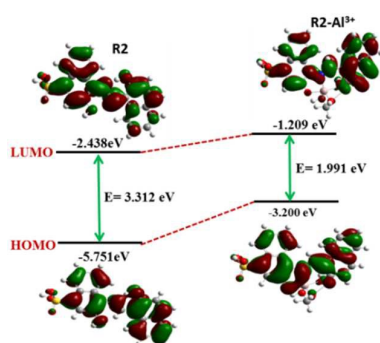


Fig.11 Energy level diagram for the frontier π -MOs of **R2** and **R2-Al³⁺**.

To enrich the practical application of **R1** and **R2** we monitored the presence of Al^{3+} on a test paper strip. For this, we prepared four test strips immersing them separately into 10.0 μM EtOH: H_2O (4:1, v/v) solution of **R1**, **R2**, **R1-Al³⁺** & **R2-Al³⁺** respectively. The test papers were then allowed to dry at room temperature. As shown in Fig. 12, the test paper strip dipped in **R1** was faint yellow and non-fluorescent while the one dipped in **R2** was yellow and blue fluorescent under visible and UV light respectively. **R1-Al³⁺** showed dark yellow colour under visible light and emit bright yellow fluorescence under UV light while **R2-Al³⁺** paper strip showed dark yellow colourimetrically and light pink fluorescent under UV light.



Fig. 12 Colorimetric and fluorescence response of test strips of **R1** / **R2** in presence of Al^{3+} .

Conclusion

Thus we have successfully presented an experimental demonstration of optical sensing of Al^{3+} by two simple Schiff bases **R1** & **R2** at the level of 10^{-8} M which indicates that our probes are highly efficient ones. Although **R1** selectively shows off/on fluorescence response with Al^{3+} , but the judicious structural changes in the basic framework of the same lead to the activation of ESIPT-blended ratiometric response of **R2** for the same purpose.

Acknowledgements

KKU gratefully acknowledges the financial support [award no. 41-330/2012(SR)] from UGC, New Delhi. Shweta acknowledges the financial support from UGC, New Delhi for JRF/SRF (Aw.No.19-12/2010 (i) EU-IV). Neeraj acknowledges UPE-JRF for research fellowship (chem./2012-13/154) and S.K.Asthana acknowledges CSIR, New Delhi for JRF/SRF (Aw.No.09/013 (0475)/2012-EMR-I).

References

- S. S. T. Mukherjee, B. Chattopadhyay, A. Moirangthem, A. Basu, J. Marek and P. Chattopadhyay, *Analyst*, 2012, **137**, 3975.
- B. Juskowiak, *Anal Bioanal Chem*, 2011, **399**, 3157.
- G. Frantzois, B. Galatis, P. Apostolak, *New Phytol.*, 2000, **145**, 211
- (a) E. Delhaize and P. R. Ryan, *Plant Physiol.*, 1995, **107**, 315; (b) C. Stephen, W. Smith, S. Heng, H. Ebendorff-Heidepriem, D.A.Abell, T.M. Monro, *Langmuir*, 2011, **27**, 5680.
- (a) A. A. MOSHTAGHIE, *Medical journal of the Islamic Republic of Iran*, 1993, **7**, 1372; (b) R.A. Yokel, *Neurotoxicology*, 2000, **21**, 81
- (a) D. P. Perl, A. R. Brody, *Science*, 1980, **208**, 297; (b) J.R. Walton, *Neuro. Toxicol.*, 2006, **27**, 385; (c) D. P. Perl, *Environmental Health Perspectives*, 1985, **63**, 149.
- J. Barcelo and C. Poschenrieder, *Environ. Exp. Bot.*, 2002, **48**, 75.
- (a) S. Das, S. Goswami, K. Aich, K. Ghoshal, C. K. Quah, M. Bhattacharyya and H.-K. Fun, *New J. Chem*, DOI: 10.1039/c5nj01468a; (b) X. Sun, Y. W. Wang, Y. Peng, *Org. Lett.*, 2012, **14**, 3420; (c) X. Jiang, B. Wang, Z. Yang, Y. Liu, T. Li, Z. Liu, *Inorg. Chem. Commun.*, 2011, **14**, 1224; (d) S. Sathish, G. Narayan, N. Rao, C. Janardhana, *J Fluoresc*, 2007, **17**, 1; (e) W. Cao, X. -J. Zheng, J. -P. Sun, W. -T. Wong, D. -C. Fang, J. -X. Zhang and L. -P. Jin, *Inorg. Chem.*, 2014, **53**, 3012.
- (a) Neeraj, A. Kumar, V. Kumar, R. Prajapati, S. K. Asthana, K. K. Upadhyay and J. Zhao, *Dalton Trans.*, 2014, **43**, 5831; (b) V. Kumar, A. Kumar, U. Diwan, Shweta, Ramesh, S. K. Srivastava K. K. Upadhyay, *Sensors and Actuators B*, 2015, **207**, 650; (c) Ajit Kumar, Virendra Kumar, K. K. Upadhyay, *Analyst*, 2013, **138**, 1891
- (a) S. Das, A. Sahana, A. Banerjee, S. Lohar, D. A. Safin, M. G. Babashkina, M. Bolte, Y. Garcia, I. Hauli, S. K. Mukhopadhyay, D. Das, *Dalton Trans.*, 2013, **42**, 4757;(b)

- Soojin Kim, Jin Young Noh, Ka Young Kim, Jin Hoon Kim, Hee Kyung Kang, Seong-Won Nam, So Hyun Kim, Sungsu Park, Cheal Kim, Jinheung Kim, *Inorg. Chem.* 2012, **51**, 3597; (c) Chang-Hung Chen, De-Jhong Liao, Chin-Feng Wan, An-Tai Wu, *Analyst*, 2013, **138**, 2527; (d) Hongde Xiao, Kun Chen, Nannan Jiang, Dandan Cui, Gui Yin, Jie Wang, Ruiyong Wang, *Analyst*, 2014, **139**, 1980.
11. D. Maity and T. Gobindoraju, *Chem. Commun.*, 2012, **48**, 1039.
 12. Z. Liu, W. He and Z. Guo, *Chem. Soc. Rev.*, 2013, **42**, 1568.
 13. (a) M. M. Henary, Y. Wu and C. J. Fahrni, *Chem.–Eur. J.*, 2004, **10**, 3015; (b) M. M. Henary and C. J. Fahrni, *J. Phys. Chem. A*, 2002, **106**, 5210; (c) J. E. Kwon, S. Lee, Y. You, K. -H. Baek, K. Ohkubo, J. Cho, S. Fukuzumi, I. Shin, S. Y. Park and W. Nam, *Inorg. Chem.*, 2012, **51**, 8760
 14. (a) G. Q. Yang, F. M.-Savary, Z. K. Peng, S. K. Wu and J. P. Fouassier, *Chem. Phys. Lett.*, 1996, **256**, 536; (b) Z. M. Li and S. K. Wu, *J. Fluoresc.*, 1997, **7**, 237; (c) P. F. Wang and S. K. Wu, *J. Photochem. Photobiol. A*, 1995, **86**, 109.
 15. Zhipeng Liu, Weijiang He, Zijian Guo, *Chem. Soc. Rev.*, 2013, **42**, 1568.
 16. (a) K. K. Upadhyay and A. Kumar, *Org. Biomol. Chem.*, 2010, **8**, 4892; (b) S. M. Hossain, A. Lakma, R. N. Pradhan, A. Chakraborty, A. Biswas and A. K. Singh, *RSC Adv.*, 2015, **5**, 63338; (c) J. S. Wu, W. M. Liu, X. Q. Zhuang, F. Wang, P. F. Wang, S. L. Tao, X. H. Zhang, S. K. Wu and S. T. Lee, *Org. Lett.*, 2007, **9**, 33.
 17. (a) N. Singh, M. S. Hundal, G. Hundal and M. M. Ripoll, *Tetrahedron*, 2005, **61**, 7796; (b) Singh, N.; Kumar, M.; Hundal, G. *Inorg. Chim. Acta* 2004, **14**, 4286; (c) Sougata Sinha, Rik Rani Koner, Sunil Kumar, Jomon Mathew, Monisha P. V., Imran Kazi, Subrata Ghosh, *RSC Advances*, 2013, **3**, 345; (d) Dharmaraj Jeyanthi, Murugan Iniya, Karupiah Krishnaveni, Duraisamy Chellappa, *RSC Adv.*, 2013, **3**, 20984.
 18. (a) S. Das, S. Goswami, K. Aich, K. Ghoshal, C. K. Quah, M. Bhattacharyya and H. -K. Fun, *New J. Chem.*, 2015, 39, 8582; (b) Seul Ah Lee, Ga Rim You, Ye Won Choi, Hyun Yong Jo, Ah Ram Kim, Insup Noh, Sung-Jin Kim, Youngmee Kim, Cheal Kim, *Dalton Trans.*, 2014, 43, 6650.
 19. J. M.-Sosa, M. Vinkovi, D. Vikić-Topić, *Croat. Chem. Acta*, 2006, **79**, 489.
 20. (a) Hem Joshi, Fadhil S. Kamounah, Cees Gooijer, Gert van der Zwan, Liudmil Antonov, *Journal of Photochemistry and Photobiology A: Chemistry*, 2002, **152**, 183; (b) P. Fita, E. Luzina, T. Dziembowska, D. Kopec', P. Piątkowski, Cz.Radzewicz, A. Grabowska, *Chemical Physics Letters* 2005, **416**, 305; (c) Liudmil Antonov, Walter M. F. Fabian, Daniela Nedeltcheva, Fadhil S. Kamounah, *J. Chem. Soc., Perkin Trans.*, 2000, **2**, 1173; (d) Asuka Ohshima, Atsuya Momotake, Tatsuo Arai, *Journal of Photochemistry and Photobiology A: Chemistry*, 2004, **162**, 473; (e) S.H. Alarcón, A.C. Olivieri, G.R. Labadie, R.M. Cravero, M. Gonzales-Sierra, *Tetrahedron*, 1995, **51**, 4619.
 21. (a) O. Alici, S. Erdemir, *Sensors and Actuators B*, 2015, **208**, 159; (b) Jin Young Noh, Soojin Kim, In Hong Hwang, Ga Ye Lee, Juhye Kang, So Hyun Kim, Jisook Min, Sungsu Park, Cheal Kim, Jinheung Kim, *Dyes and Pigments*, 2013, **99**, 1016.
 22. (a) IUPAC, *Spectrochim. Acta Part B*, 1978, **33**, 242; (b) USEPA, Appendix B to Part 136-Definition and Procedure for the Determination of the Method Detection Limit-Revision 1.11, Federal Register 49 (209), 43430, October 26, 1984. Also referred to as "40 CFR Part 136".
 23. M. J. Frisch, et al., Gaussian 03, Revision D.01, Gaussian, Inc., Wallingford, CT, 2004.

Graphical Abstract

